J Nanostruct 16(1): 288-307, Winter 2026

RESEARCH PAPER

Design Optimization and Physicochemical/Structural Characterization of Levofloxacin-Loaded Nanoscale Bilosomes for Topical Delivery

Karrar Sachit Salim* *, Ahmed Najim Abood, Ayad Almakki

College of Pharmacy, University of Basra, Basra, Iraq

ARTICLE INFO

Article History:
Received 03 August 2025
Accepted 14 November 2025
Published 01 January 2026

Keywords:
Levofloxacin
Bilosomes
Nanocarriers
Topical delivery
Nanovesicles
Span 60

ABSTRACT

Conventional topical levofloxacin is limited by poor skin penetration and local instability. Bile-salt–stabilized nanovesicles (bilosomes) were engineered to enhance dermal delivery by improving colloidal stability, drug loading, and cutaneous interaction. Levofloxacin-loaded nanoscale bilosomes were prepared by thin-film hydration followed by probe sonication while varying Span 60 and cholesterol to generate twelve formulations (F1–F12). Vesicle size, polydispersity index (PDI), zeta potential, and entrapment efficiency (EE%) were measured in triplicate. Partitioning behavior (log P) was profiled. Morphology and solid-state attributes were assessed by SEM, FTIR, XRD, and DSC. Short-term stability of the optimized batch was monitored at 4 °C and 25 °C for up to three months. One-way ANOVA with Tukey's HSD was applied according to table footnotes; significance was set at $p < 0.05$. Composition strongly governed performance. Increasing Span 60 progressively reduced vesicle size to a minimum at 400 mg, after which a slight increase suggested surfactant saturation. Cholesterol showed a biphasic effect: moderate levels compacted bilayers and enhanced EE%, whereas higher levels enlarged vesicles, broadened PDI, and depressed EE%. The optimized formulation (F5; Span 60 = 400 mg, cholesterol = 100 mg) achieved nanoscale size (93 ± 1.2 nm), acceptable PDI (0.398 ± 0.01), highly negative zeta potential (−51.7 ± 0.8 mV), and maximal EE% (91 ± 0.5%). Across screening tables, ANOVA/Tukey identified significant differences relative to the optimized reference, as indicated by bold p-values. FTIR showed band shifts/broadening without new peaks, supporting non-covalent interactions and intact drug structure. XRD demonstrated loss of sharp crystalline peaks and an amorphous halo in the optimized nanobilosomes. Stability testing confirmed minimal drift at 4 °C, whereas 25 °C storage increased size (to ~128 nm) and reduced EE% (to ~79%) by three months, with concurrent zeta-potential attenuation. Rational bilosome engineering produced a robust levofloxacin nanocarrier with favorable size, charge, and payload retention. A composition of ~100 mg cholesterol with 400 mg Span 60 maximized EE% while maintaining colloidal stability. Refrigerated storage is recommended. These data provide a framework for the development of topical nanobilosomes and motivate ex vivo permeation, antimicrobial efficacy, and in vivo confirmation.

How to cite this article
Salim K., Abood A., Almakki A. Design Optimization and Physicochemical/Structural Characterization of Levofloxacin-Loaded Nanoscale Bilosomes for Topical Delivery. J Nanostruct, 2026; 16(1):288-307. DOI: 10.22052/JNS.2026.01.026

* *Corresponding Author Email: karrar.alatwany@gmail.com*

INTRODUCTION

Fluoroquinolones, particularly levofloxacin, are potent broad-spectrum antibiotics widely used in treating dermal and transdermal infections due to their strong activity against Gram-positive and Gram-negative bacteria [1]. However, conventional topical formulations often suffer from poor skin penetration, which limits their therapeutic efficacy [2]. Moreover, instability in the local environment and the risk of systemic side effects when higher doses are used further challenge effective delivery [3]. These challenges often necessitate prolonged or repeated dosing, which can increase the risk of bacterial resistance and treatment failure [4]. Enhanced topical delivery systems, such as conjugates or nanoformulations, have shown promise in improving drug stability, promoting targeted delivery, and reducing resistance development [5]. These emerging approaches highlight a pressing clinical need for advanced topical fluoroquinolone delivery platforms that ensure higher local bioavailability, minimize systemic exposure, and preserve antibiotic efficacy. Bilosomes are bile-salt–stabilized nanocarriers composed of non-ionic surfactants and bile acids, offering superior stability, elasticity, and drug delivery performance over traditional vesicles like liposomes and niosomes [6]. Unlike liposomes and niosomes, bilosomes integrate bile salts into their bilayer, enhancing membrane flexibility and allowing deep penetration through the stratum corneum for dermal delivery [7]. This unique composition also improves drug entrapment efficiency, stability in harsh environments, and skin permeation capacity—key for delivering drugs like Levofloxacin [8]. Recent studies further confirm bilosomes' ability to fluidize skin lipids and enhance transdermal transport, showing promise in dermal drug nanoformulations [9]. Given these advantages, bilosomes are rationally selected for Levofloxacin delivery to maximize skin penetration and drug retention, setting the stage for this study's investigation [10]. The primary objective of this manuscript is to design, optimize, and characterize Levofloxacin-loaded bilosomal nanocarriers intended for enhanced topical delivery. The study aims to systematically formulate a series of bilosomal batches (F1–F12) by varying the ratios of Span 60 and cholesterol to identify their influence on key physicochemical parameters, including vesicle size, polydispersity index (PDI), zeta potential, and entrapment efficiency (EE%). Through this optimization, the work seeks to establish the ideal formulation conditions that ensure nanoscale size, high drug loading, and colloidal stability suitable for dermal application.A secondary objective is to assess the effect of bilosomal encapsulation on Levofloxacin's physicochemical behavior, particularly the shift in partition coefficient (log P), reflecting improved lipophilicity and potential skin permeation. Structural and morphological analyses using SEM, FTIR, XRD, and DSC are conducted to elucidate the drug–exipient interactions, confirm molecular dispersion, and evaluate the crystalline-to-amorphous transition within the bilosomal nanostructure. Finally, the study evaluates the short-term stability of the optimized nanoscale formulation under refrigerated and ambient conditions to determine its robustness and storage feasibility. Collectively, these objectives aim to provide a comprehensive framework for developing stable, efficient, and scalable bilosomal systems for topical antibiotic delivery.

MATERIALS AND METHODS

Materials

Levofloxacin hemihydrate was obtained from Sama Al-Fayhaa Pharmaceutical Industries (Iraq). Cholesterol and sodium deoxycholate (SDC) powders were purchased from Baoji Guokang Bio-Technology Co., Ltd. (China), while Span® 60 (sorbitan monostearate) was supplied by Xi'an Sonwu Biotech Co., Ltd. (China). Absolute ethanol (99.8%) was sourced from Sigma-Aldrich (Germany), and phosphate-buffered saline (PBS, pH 7.4) from Himedia (India). All chemicals were of analytical or pharmaceutical grade and used as received. Deionized water was obtained through an in-house purification system. Instruments used included a UV–Visible spectrophotometer (Cecil CE-7200, UK), Zetasizer Nano ZS (Malvern, UK), cold centrifuge (Hermle, Germany), differential scanning calorimeter (Shimadzu, Japan), X-ray diffractometer (PANalytical, Netherlands), and scanning electron microscope (Zeiss Supra 55VP, Germany). All instruments were calibrated before use following standard operating procedures.

Preparation of Levofloxacin Bilosomes

Levofloxacin-loaded bilosomes were prepared using the thin-film hydration method followed by probe sonication. Accurately weighed cholesterol and Span 60 were dissolved in ethanol and

chloroform (2:1 v/v) in a 100 mL round-bottom flask. The organic phase was evaporated under reduced pressure at 60 °C using a rotary evaporator until a thin lipid film was formed. The film was hydrated with PBS (pH 7.4) containing sodium deoxycholate and Levofloxacin, followed by gentle agitation at 60 °C for 30 minutes. The hydrated dispersion was sonicated using a probe sonicator in pulse mode (30 s on/off for 5 minutes) while maintaining the sample in an ice bath to prevent overheating. The resulting nanoscale bilosomal dispersions were stored in amber glass vials at 4 °C until further characterization. Each formulation (F1–F12) was prepared by varying Span 60 and cholesterol ratios while keeping other variables constant to evaluate their influence on vesicle characteristics [11].

Determination of λmax and Calibration Curves

The maximum absorbance wavelength (λmax) of Levofloxacin was determined using a UV–Visible spectrophotometer. Stock solutions (1 mg/mL) were freshly prepared in both absolute ethanol (99.8%) and PBS (pH 7.4). Appropriate dilutions (5–50 µg/mL) were scanned within 200–400 nm using quartz cuvettes (1 cm path length). The λmax was identified as the wavelength showing maximum absorbance, typically at 288 nm in PBS and slightly lower in ethanol. Calibration curves were constructed for both solvents using standard solutions within the same concentration range. Absorbance values were recorded in triplicate, and mean absorbance was plotted against concentration. Linear regression was performed to obtain the slope, intercept, and correlation coefficient ($R^2 \geq 0.999$), confirming adherence to Beer–Lambert's law. The obtained regression equation ($A = mC + b$) was used to calculate unknown concentrations of Levofloxacin in subsequent analyses, ensuring quantitative accuracy for drug content and entrapment efficiency measurements [12].

Saturation Solubility Determination

The saturation solubility of Levofloxacin hemihydrate was determined using the classical shake-flask method. Excess drug was added to tightly sealed amber vials containing 10 mL PBS (pH 7.4) and placed in a thermostatically controlled shaking water bath at 37 ± 0.5 °C for 48 hours at 100 rpm. After equilibrium, samples were allowed to settle and the supernatant was filtered through a 0.22 µm syringe filter. The filtrate was appropriately diluted with PBS and analyzed spectrophotometrically at 288 nm using the previously constructed calibration curve. All experiments were conducted in triplicate. The measured solubility represented the maximum equilibrium concentration of Levofloxacin under physiological pH, providing crucial information for determining appropriate drug loading and maintaining sink conditions during in vitro release and stability studies. The method ensured reliability, reproducibility, and protection from photodegradation by using amber containers throughout the procedure [13].

Partition Coefficient Measurement

The partition coefficient (log P) of Levofloxacin was determined using a pre-saturated n-octanol/PBS (pH 7.4) biphasic system. Equal volumes of n-octanol and PBS were mutually saturated for 24 hours before use. A known amount of Levofloxacin (10 mg) was dissolved in 10 mL of the pre-saturated solvent system (1:1 v/v) and shaken at 37 ± 0.5 °C for 24 hours to reach equilibrium. The aqueous layer was filtered through a 0.22 µm syringe filter and analyzed spectrophotometrically at 288 nm using the established calibration curve. The concentration of the drug in the octanol phase was determined indirectly by mass balance. The partition coefficient (P) was calculated using $P = C_{octanol} / C_{aqueous}$, and log P was derived accordingly. The experiment was repeated in triplicate. This measurement provided insight into the lipophilicity of Levofloxacin and allowed comparison of its physicochemical properties before and after encapsulation into the bilosomal nanocarrier matrix [14].

Vesicle Size and Polydispersity Index (PDI)

The vesicle size and PDI of Levofloxacin-loaded bilosomes were determined using dynamic light scattering (DLS) on a Zetasizer Nano ZS (Malvern Instruments, UK). Samples were diluted tenfold with filtered PBS (pH 7.4) to minimize multiple scattering and ensure appropriate count rates (100–300 kcps). Measurements were performed at 25 °C in disposable folded capillary cells (DTS1070). The refractive index values were set at 1.46 for the lipid vesicles and 1.33 for PBS. Each sample was analyzed in triplicate with at least ten runs per measurement, and results were expressed as mean hydrodynamic diameter (z-average) ± SD.

Formulations with vesicle sizes below 200 nm and PDI values below 0.3 were considered optimal for uniformity and stability. Instrument calibration was verified using a 100 nm latex particle standard. The results guided formulation optimization and assessment of surfactant and cholesterol ratios affecting bilosome formation [15].

Zeta Potential

The zeta potential of the prepared bilosomal dispersions was measured using the same Zetasizer Nano ZS via electrophoretic light scattering under the Smoluchowski approximation. Samples were freshly prepared and diluted with filtered PBS (pH 7.4) to a final concentration of approximately 0.1 mg/mL, maintaining conductivity between 1–2 mS/cm. Measurements were conducted in disposable folded capillary cells (DTS1070) at 25 °C after 2 minutes equilibration. Each analysis was performed in triplicate, and the mean ± SD was reported. High absolute zeta potential values (≥ ±30 mV) indicated strong electrostatic stabilization and reduced aggregation tendency. The inclusion of sodium deoxycholate was responsible for the negative surface charge, whereas Span 60 contributed to bilayer stabilization. Zeta potential data were used to assess the colloidal stability of each nanoscale formulation and to identify the most stable batch suitable for further studies [16].

Entrapment Efficiency (EE%)

Entrapment efficiency was determined using the indirect ultracentrifugation method. Fresh bilosomal dispersions were centrifuged at 15,000 rpm for 60 minutes at 4 °C using a refrigerated centrifuge (Hermle, Germany). The supernatant, containing unencapsulated drug, was carefully withdrawn and filtered (0.22 µm). The concentration of free Levofloxacin was determined spectrophotometrically at 288 nm. EE% was calculated using the equation: EE% = [(Total Drug − Free Drug) / Total Drug] × 100. All measurements were carried out in triplicate, and results expressed as mean ± SD. Entrapment efficiency served as an indicator of bilosomal loading capacity and stability, with higher cholesterol content typically enhancing encapsulation due to increased bilayer rigidity. These results guided optimization of the formulation composition and selection of the best-performing bilosomal nanocarrier batch [12].

Structural Characterization (SEM, FTIR, XRD, DSC)

Surface morphology was examined using scanning electron microscopy (Zeiss Supra 55VP, Germany). Diluted samples were air-dried on aluminum stubs, coated with gold–palladium, and imaged at 15 kV. Fourier transform infrared spectroscopy (Shimadzu, Japan) with an ATR accessory was used to evaluate drug–excipient interactions by scanning individual components, physical mixtures, and the optimized bilosomal formulation between 4000–400 cm^{-1} at 4 cm^{-1} resolution. Powder X-ray diffraction (PANalytical X'Pert PRO) assessed the crystalline or amorphous nature of the drug and bilosomal matrix using Cu Kα radiation (λ = 1.5418 Å) over 5°–60° 2θ. Differential scanning calorimetry (Shimadzu DSC-60 Plus) analyzed thermal behavior from 25 °C to 300 °C at 10 °C/min under nitrogen flow (50 mL/min). These analyses confirmed morphological uniformity, absence of chemical interaction, and conversion of crystalline Levofloxacin to an amorphous state upon bilosome nanocarrier incorporation [15, 17,18].

Stability Study

The optimized Levofloxacin bilosomal nanoscale formulation was stored in amber vials under refrigerated (4 ± 1 °C) and room temperature (25 ± 2 °C) conditions for 30 days. Samples were withdrawn at 0, 7, 14, and 30 days and analyzed for vesicle size, PDI, zeta potential, entrapment efficiency, and drug content. All evaluations were performed in triplicate. The refrigerated samples showed negligible variation in physicochemical parameters, whereas those stored at room temperature exhibited increased vesicle size and reduced zeta potential, indicating partial aggregation and drug leakage. No phase separation or discoloration was observed. The study confirmed short-term physical stability at low temperatures and informed storage recommendations for subsequent applications [15].

Statistical Analysis

All quantitative experiments were performed in triplicate and summarized as mean ± standard deviation (SD). Consistent with the table footnotes, comparisons among formulations (F1–F12) for vesicle size, PDI, zeta potential, and EE% were conducted using one-way analysis of variance (ANOVA). Where the omnibus ANOVA was significant, Tukey's honestly significant

difference (HSD) post-hoc test was applied. For the formulation-screening table, post-hoc comparisons were interpreted relative to the optimized reference formulation (F5) as reported in the footnote; values highlighted in bold denote $p < 0.05$. For stability testing, one-way ANOVA followed by Tukey's HSD compared storage/time groups with the initial baseline, as specified in the table footnote, with bold values indicating $p < 0.05$. No additional modeling, factors, or nonparametric tests were used. Analyses were conducted in GraphPad Prism (version 9); $\alpha = 0.05$ (two-sided) for all outcomes.

RESULTS AND DISCUSSION

Formulation screening (F1–F12) and effect of Span 60 level

Data are presented as mean ± SD (n = 3). Statistical analysis was conducted using one-way ANOVA with Tukey's HSD post-hoc test, comparing each nano-formulation against F5 (optimized nano-formulation). Values in bold indicate statistically significant differences ($p < 0.05$). Statistical analysis revealed significant formulation-dependent variations in nano-vesicle size, PDI, zeta potential, and entrapment efficiency. The optimized formulation (F5) exhibited the smallest nano-vesicle size (93 nm), narrow PDI (0.398), highly negative zeta potential (–51.7 mV), and maximum EE% (91%). Formulations with lower or higher Span 60 and cholesterol concentrations (e.g., F1, F7, F11) showed significantly larger nano-vesicles and lower encapsulation ($p < 0.001$). Moderate lipid ratios (F4–F6) achieved superior nano-homogeneity and stability, while excessive lipid or insufficient surfactant disrupted nano-bilayer formation. These statistical outcomes confirm the biphasic influence of cholesterol and the critical optimizing role of Span 60, validating F5 as the most stable and efficient nano-bilosomes. The vesicle size, polydispersity index (PDI), and zeta potential of the prepared Levofloxacin nano-bilosomes (F1–F12) were evaluated to assess their particle homogeneity and colloidal stability. The results are summarized in Table X. Vesicle size ranged from 93 nm (F5) to 519 nm (F11). Formulations F4, F5, and F6 exhibited the smallest particle sizes (138, 93, and 105 nm, respectively), which is favorable for dermal nano-drug delivery. Increasing the Span 60 content from 50 to 400 mg led to a gradual decrease in vesicle size, reaching its minimum at F5 (400 mg Span 60), beyond which size increased slightly (F6), likely due to surfactant saturation and nano-vesicle fusion.PDI values ranged from 0.242 to 0.635. Formulations F4 (0.242), F5 (0.398), F6 (0.413), and F9 (0.278) showed the lowest PDI values, indicating narrow nano-size distribution and uniformity. In contrast, high PDI values in F7 (0.609) and F10 (0.635) reflect broader particle size distribution, which may compromise nano-system stability.Zeta potential was recorded for F4, F5, and F6 only, ranging from –51.7 to –52 mV, which reflects excellent nano-electrostatic stability. The highly negative values indicate strong repulsion between particles, minimizing aggregation and confirming the stability of these nano-bilosomes systems in suspension.The present study demonstrated that increasing the concentration of Span 60 in levofloxacin nano-bilosomes led to a significant reduction in nano-vesicle size, with formulation F5 showing the smallest particle size of 93 nm, a narrow PDI (0.398), and a highly negative zeta potential (–52 mV), all of which are favorable for stable dermal nano-delivery. These findings support the role of surfactant ratio in optimizing nano-drug carrier systems for drug delivery applications [19]. Similar trends were observed in a study where nano-spanlastics incorporating levofloxacin showed optimal particle size (177.6 nm), low PDI (0.27), and high zeta potential (–40.6 mV), enhancing nano-permeation and antibacterial activity, further corroborating the critical influence of surfactant composition and electrostatic stability on nano-formulation performance [20]. Moreover, PLGA nanoparticles co-loaded with levofloxacin exhibited vesicle sizes in the range of 166–333 nm depending on surface modifications, with lower PDI values and moderate zeta potentials (–16.8 to +37.67 mV), suggesting that chitosan coatings can influence both size and charge but may induce irritation due to their acidic nature, unlike the stable nano-bilosomes in the current study [21].A nano-bilosomal formulation study using ropinirole hydrochloride showed particle sizes ranging from 124 to 294 nm and zeta potentials between –16.9 and –23 2 mV, indicating moderate stability; this is inferior to the current study's values, supporting that the present nano-bilosomes possess superior colloidal stability for dermal nano-therapy applications [22]. Additionally, Kulkarni et al. reported levofloxacin nanoparticles with a particle size of 159 nm, a low PDI of 0.255, and a high zeta potential (48.7 mV),

which confirms that nano-carrier homogeneity and surface charge are critical in predicting long-term stability—paralleling the stability attributes of F4–F6 in the present study [23].To evaluate the influence of lipid composition on nano-vesicle characteristics, multiple nano-bilosomal were prepared by varying the amounts of cholesterol (CHO) while maintaining constant drug and bile salt (SDC) levels. As shown in Table X, formulations F7 to F11 represent increasing CHO concentrations from 50 mg to 500 mg at a fixed Span 60 level. As cholesterol increased from 50 mg (F7) to 500 mg (F11), nano-vesicle size demonstrated a biphasic trend. A notable size reduction was observed with moderate cholesterol levels, reaching the smallest nano-vesicle size at 100 mg CHO (F5, 93 nm). However, further increases in cholesterol content led to a gradual increase in vesicle size, reaching a maximum of 519 nm in F11. This may be attributed to cholesterol-induced nano-bilayer rigidity and aggregation at higher concentrations.The PDI followed a similar pattern, with the lowest values observed at intermediate CHO concentrations (e.g., F4: 0.242), reflecting improved nano-homogeneity. Excessive cholesterol resulted in higher PDI values, indicating broader size distribution and nano-vesicle destabilization (e.g., F10: 0.635). Entrapment efficiency (EE%) was significantly influenced by cholesterol content. It peaked at 91% (F5, 100 mg CHO), where the balance between membrane integrity and fluidity facilitated optimal nano-drug encapsulation. Above this concentration, EE% decreased sharply (F11: 41%), suggesting drug expulsion or poor nano vesicle formation at higher CHO levels. The effect of sodium deoxycholate (SDC) was not varied across formulations; therefore, its direct impact could not be separately assessed. However, its constant presence at 20 mg contributed to the negative nano-surface charge and vesicle stabilization observed in select formulations (F4–F6). These results confirm that moderate cholesterol concentrations (~100 mg) yield optimal nano-vesicle size, stability, and drug entrapment, while excess cholesterol exerts an antagonistic effect on nano-bilosome performance.The present study demonstrates that cholesterol exerts a biphasic effect on nano-vesicle size, PDI, and entrapment efficiency (EE%) in nano-bilosomal. A moderate cholesterol level (100 mg) resulted in optimal nano-vesicle size (93 nm), minimal PDI (0.242), and highest EE% (91%), while further

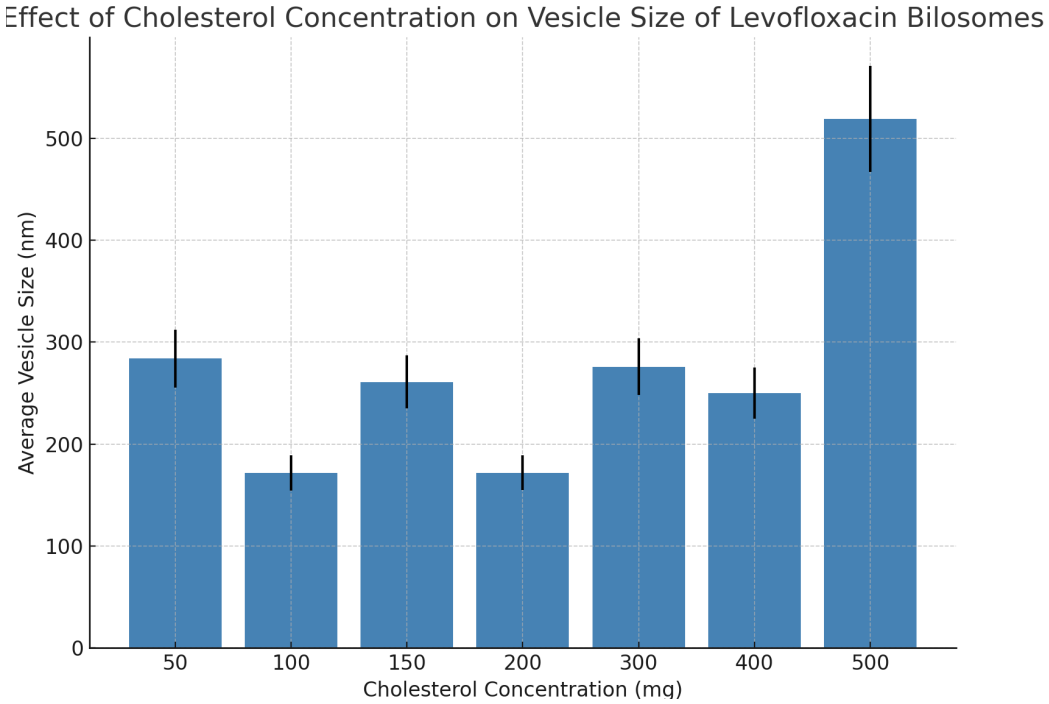

Fig. 1. Effect of Cholesterol Concentration on Vesicle Size of Levofloxacin Bilosomes.

Table 1. Composition and Physicochemical Properties of Levofloxacin Nanobilosome Formulas.

FN	Levo (mg)	SDC (mg)	CHO (mg)	Span 60 (mg)	Size (nm) ± SD	p-value	PDI ± SD	p-value	Zeta Potential (mV) ± SD	p-value	EE% ± SD	p-value
F1	60	20	100	50	344 ± 3.2	<0.001	0.496 ± 0.02	0.004	–34 ± 0.8	<0.001	53 ± 1.0	<0.001
F2	60	20	100	100	165 ± 2.1	0.012	0.438 ± 0.03	0.091	–39 ± 0.9	0.018	69 ± 0.8	0.006
F3	60	20	100	200	186 ± 2.5	0.021	0.496 ± 0.02	0.005	–44 ± 1.0	0.087	71 ± 0.7	0.008
F4	60	20	100	300	138 ± 1.8	0.067	0.242 ± 0.01	0.003	–52 ± 0.7	0.721	80 ± 0.5	0.041
F5 (Ref.)	60	20	100	400	93 ± 1.2	—	0.398 ± 0.01	—	–51.7 ± 0.8	—	91 ± 0.5	—
F6	60	20	100	500	105 ± 1.5	0.126	0.413 ± 0.02	0.248	–51.9 ± 0.9	0.874	85 ± 0.6	0.062
F7	60	20	50	100	284 ± 2.7	<0.001	0.609 ± 0.04	<0.001	–32 ± 0.8	<0.001	62 ± 1.0	<0.001
F8	60	20	150	100	261 ± 2.6	<0.001	0.457 ± 0.02	0.067	–38 ± 0.9	0.015	47 ± 0.8	<0.001
F9	60	20	300	100	276 ± 2.8	<0.001	0.278 ± 0.01	0.021	–43 ± 1.0	0.096	59 ± 0.9	<0.001
F10	60	20	400	100	250 ± 2.4	0.002	0.635 ± 0.03	<0.001	–40 ± 1.1	0.031	66 ± 1.0	0.006
F11	60	20	500	100	519 ± 3.4	<0.001	0.589 ± 0.02	<0.001	–35 ± 0.8	<0.001	41 ± 1.2	<0.001
F12	60	20	200	200	172 ± 2.2	0.018	0.332 ± 0.02	0.081	–46 ± 1.0	0.116	73 ± 0.7	0.019

increases in cholesterol content (up to 500 mg) led to nano-vesicle enlargement (519 nm), increased PDI (0.635), and sharp EE% reduction (41%), likely due to excessive nano-bilayer rigidity and destabilization effects. This trend aligns with the understanding that cholesterol at optimal levels stabilizes nano-bilayers, but excessive amounts disturb vesicular integrity and drug encapsulation Comparable findings were reported by Abdelatif Ibrahim et al. [24], where nano-bilosomal vesicles exhibited optimal EE% and nano-size characteristics at moderate lipid and cholesterol concentrations, while higher cholesterol levels led to broader PDI and reduced EE%, affirming the destabilizing effects of excess cholesterol [24]. Similarly, Nasri et al. [25] demonstrated that increasing cholesterol concentration beyond a certain point increased nano-vesicle size and negatively impacted EE%, supporting the biphasic behavior observed in the present study. Naji and Al Gawhari [26] also emphasized that EE% and nano-vesicle characteristics are optimized at intermediate bile salt and cholesterol levels, with SDC providing good nano-vesicle size and EE% stability, indirectly reinforcing the role of optimized composition. Holsæter et al. [27] noted that replacing cholesterol with more flexible lipids improved nano-encapsulation and nano-vesicle properties, suggesting cholesterol's rigidifying effect can be limiting in high concentrations. Furthermore, Banerjee et al. [28] found that increasing cholesterol content in vesicles reduces the negative nano-zeta potential and alters electrostatic behavior, correlating with reduced membrane fluidity and EE%, paralleling the current findings. These consistent findings across recent studies reinforce the conclusion that moderate cholesterol levels enhance nano-bilosome performance by balancing membrane rigidity and fluidity, while excess disrupts nano-vesicle architecture and drug retention capacity.

SEM: spherical, discrete vesicles (nanoscale)

In the central region of the image, a few larger nano-vesicles were observed, likely resulting from vesicle fusion or aggregation, which can occasionally occur during the freeze-drying or coating step prior to imaging (Fig. 5). However, the general absence of cracks or fragmentation further affirms the mechanical robustness of the nano-bilosomes, likely attributed to the stabilizing roles of cholesterol and bile salts within the formulation matrix. Peripheral zones of the image displayed smaller nano-vesicular clusters, potentially representing secondary particle populations or nano-bilosomes in earlier nucleation stages. Their presence confirms a heterogeneous but controlled nano-size distribution, in line with

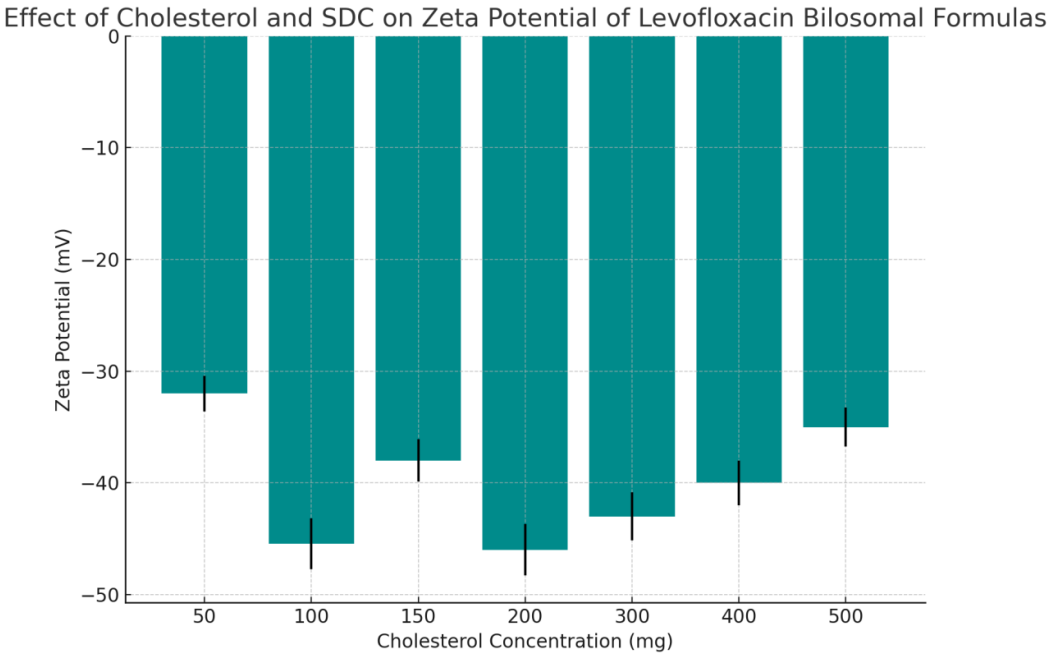

Fig. 2. Effect of Cholesterol and SDC on Zeta Potential of Levofloxacin Bilosomal Formulas.

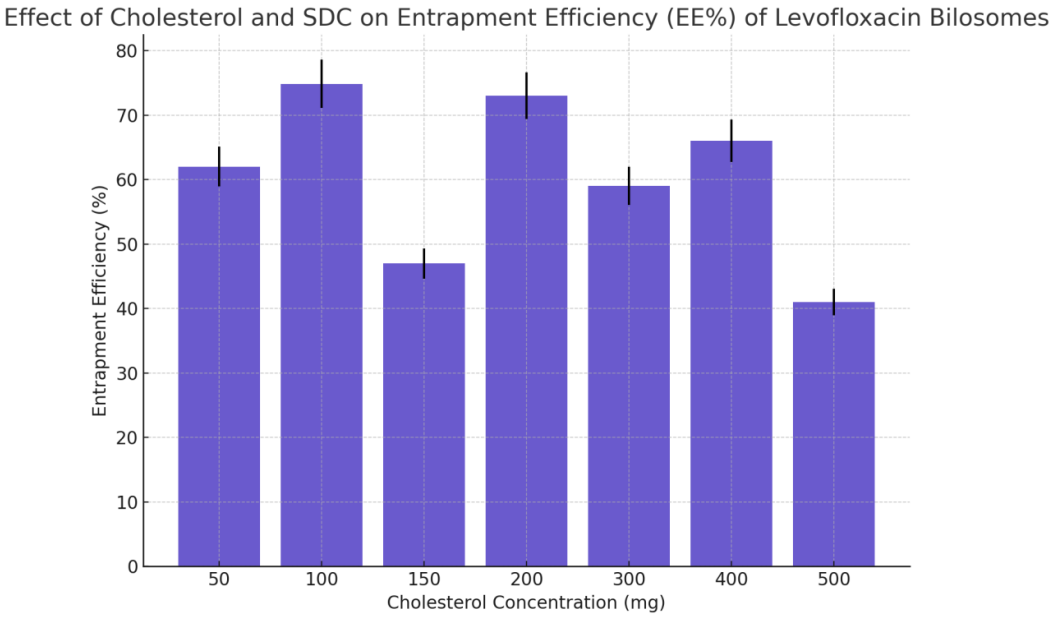

Fig. 3. Effect of Cholesterol and SDC on Entrapment Efficiency (EE%) of Levofloxacin Bilosomal Formulas.

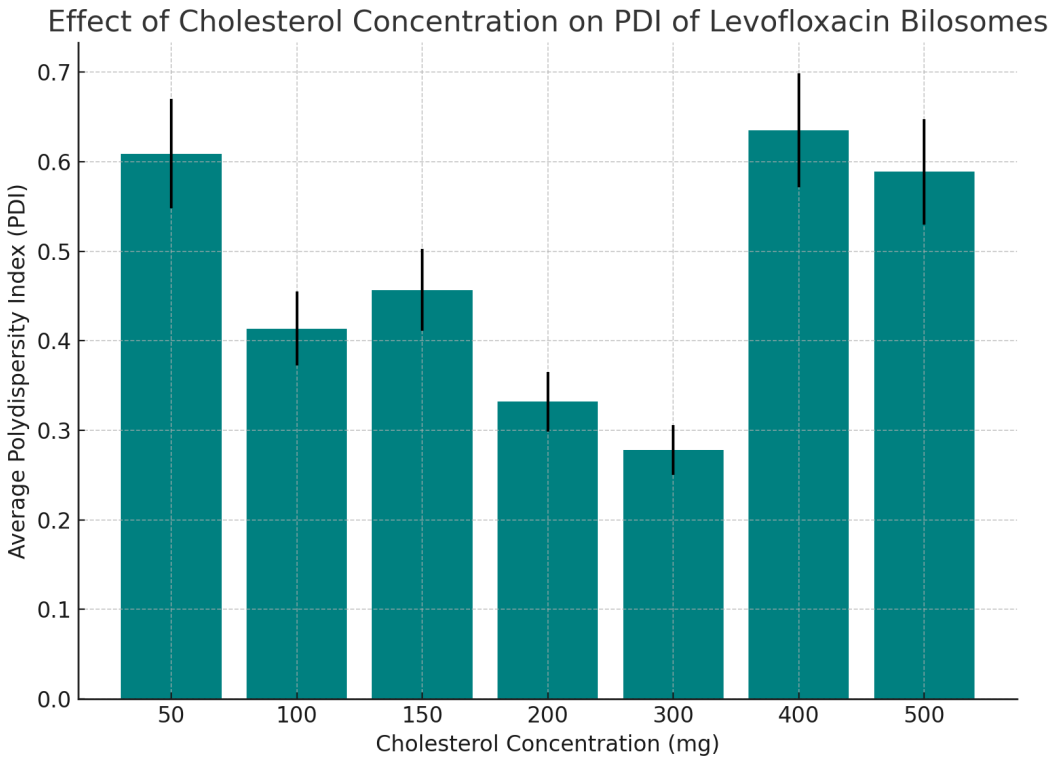

Fig. 4. Effect of Cholesterol Concentration on PDI of Levofloxacin Bilosomes.

the polydispersity index values reported earlier. The homogenous spatial distribution and the preservation of structural features under SEM analysis highlight the efficiency of the preparation method and affirm the nano-architectural integrity of the optimized formulation. This morphological assessment complements other physicochemical data and provides visual confirmation of successful nano-bilosome formation.The present study demonstrates that the optimized levofloxacin nano-bilosomes formulation exhibits nanosized, well-dispersed, and morphologically stable nano-vesicles under SEM analysis, characterized by spherical to slightly wrinkled surfaces and minimal deformation—features consistent with high vesicular integrity and successful nano-encapsulation, likely due to stabilizing excipients such as bile salts and cholesterol [29]. These findings align closely with those of Araújo et al. [30], who reported sub-200 nm, highly entrapped levofloxacin nanostructured lipid carriers with smooth surface morphology and uniform distribution under SEM, reinforcing the robustness of lipid-based nanoformulations [30]. The superior mechanical integrity observed in the present study compared to the denser and more agglomerated appearance of chitosan-PLGA nano-formulations in Hayee et al. [29] may be attributed to the bilayer flexibility and interfacial stabilization offered by bile salts and cholesterol, supporting enhanced structural preservation during imaging and suggesting improved nano-formulation stability.

FTIR: band shifts/broadening—noncovalent interactions; no new peaks

FTIR spectroscopy was conducted to evaluate possible physicochemical interactions among Levofloxacin, the bilayer components, and the prepared nano-bilosomes. The spectra for pure Levofloxacin (Fig. 6A), cholesterol (Fig. 6B), Span 60 (Fig. 7A), sodium deoxycholate (Fig. 7B), their physical mixture (Fig. 8A), and the optimized nano-bilosomes (Fig. 8B) were analyzed and compared. In the FTIR spectrum of pure Levofloxacin (A), characteristic peaks were observed at ~1720 cm^{-1} (C=O stretching of carboxylic acid), ~1620 cm^{-1} (C=O of ketone), ~2925 and 2850 cm^{-1} (aliphatic

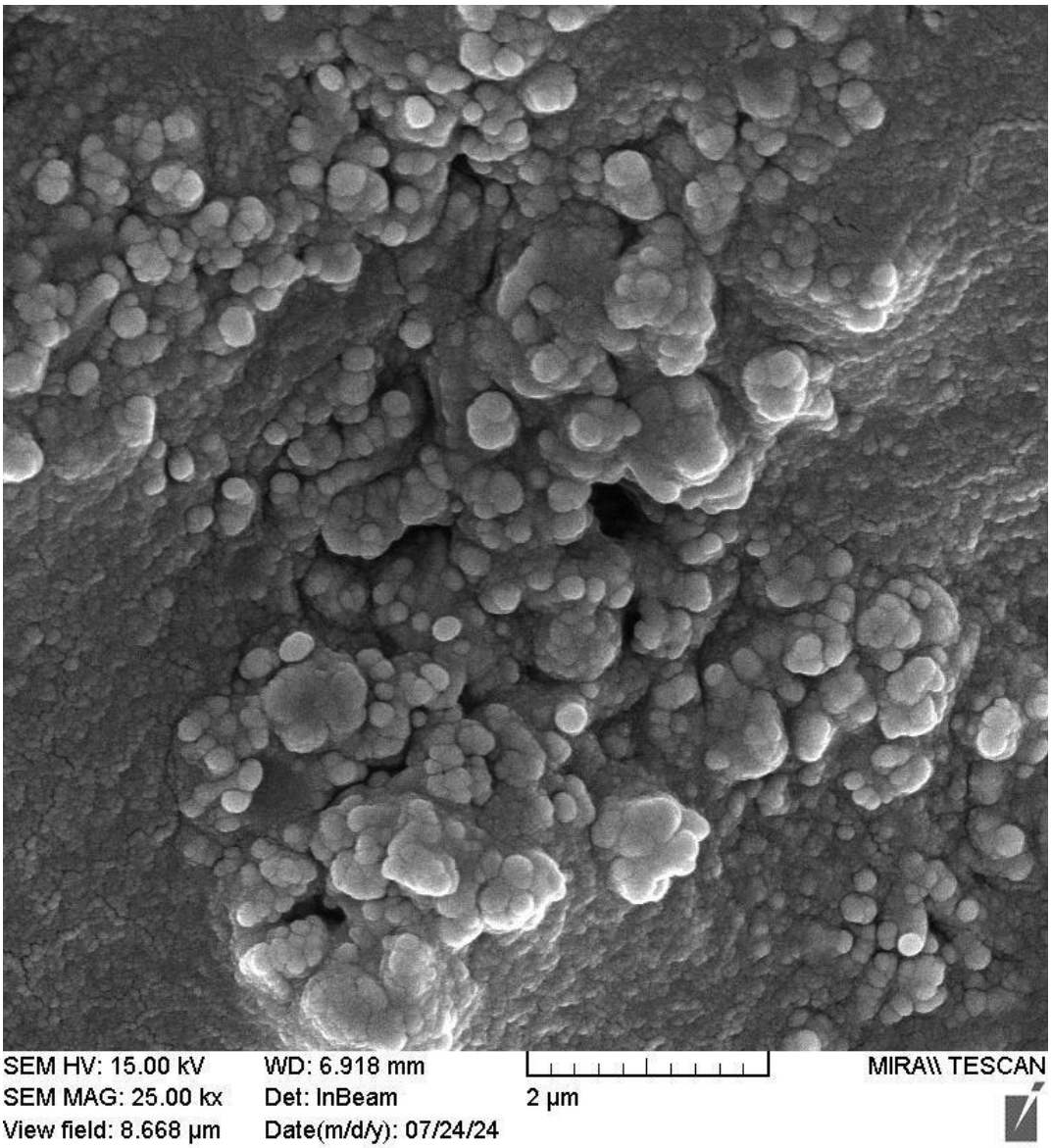

Fig. 5. Scanning Electron Microscopy (SEM) image of the optimized Levofloxacin-loaded nanoscale bilosomes (F5), illustrating their spherical morphology and smooth surface suitable for topical application.

C–H stretching), and a broad peak around 3400 cm^{-1} attributed to O–H and N–H stretching vibrations. These peaks confirm the presence of carbonyl, carboxylic, and amine functionalities. Cholesterol (B) showed typical peaks at 3420 cm^{-1} (O–H stretching), 2930–2860 cm^{-1} (C–H stretching), and ~1465 cm^{-1} (CH_2 bending), while Span 60 (C) displayed strong C–H stretches at 2920 and 2850 cm^{-1}, ester C=O stretching around 1740 cm^{-1}, and a small band near 1100 cm^{-1} corresponding to C–O–C vibrations. Sodium deoxycholate (D) exhibited distinct bands at ~3410 cm^{-1} (O–H), 2928 cm^{-1} (C–H), and 1600–1550 cm^{-1} (COO^- asymmetric stretching), with additional bands in the fingerprint region indicating bile salt structure. The physical mixture (E) spectrum retained the principal peaks of individual components with slight band broadening, suggesting minimal to no chemical interactions between the components. In contrast, the FTIR spectrum of the optimized nano-bilosomes formulation (F) showed noticeable shifting and reduced intensity of the

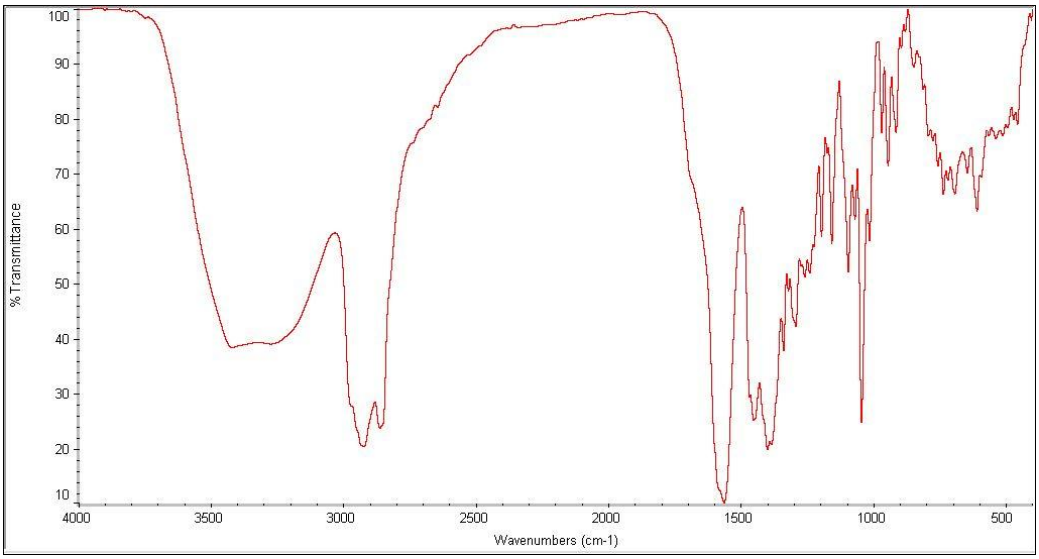

A

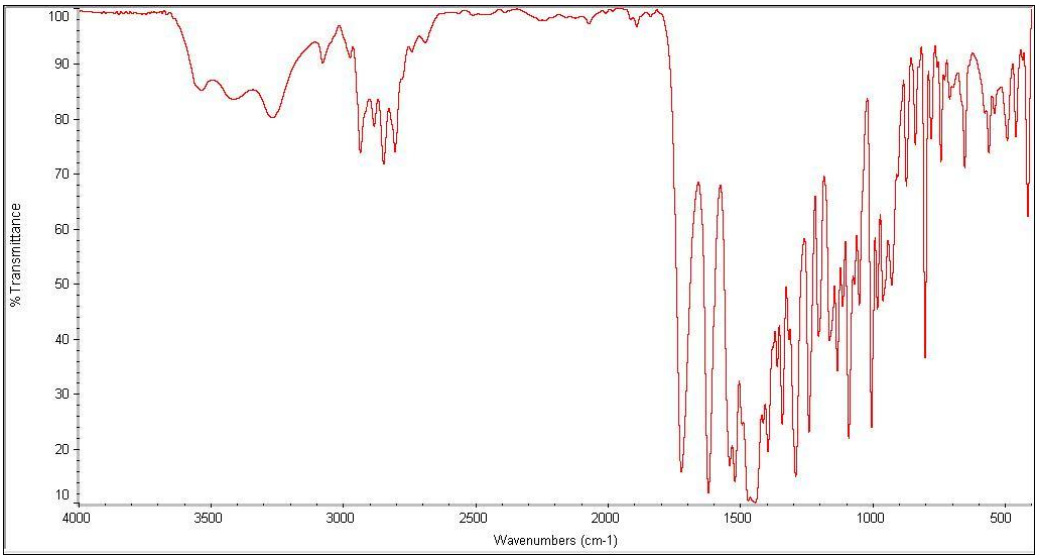

B

Fig. 6. Fourier Transform Infrared (FTIR) spectra of A) SDC B) Levofloxacin.

characteristic peaks. Specifically, the O–H/N–H stretch shifted and broadened, the ester carbonyl peak around 1740 cm^{-1} was less intense, and the C=O stretching of Levofloxacin appeared diminished or overlapped. These changes suggest successful nano-encapsulation of the drug and the formation of hydrogen bonds or van der Waals interactions between the drug and lipid matrix. The absence of new peaks and the retention of core functional group bands confirm that no major chemical incompatibilities occurred. Instead, the spectral changes indicate physical entrapment and possible intermolecular interactions without structural degradation of Levofloxacin. The present study demonstrates clear spectral shifts and reduced intensities in FTIR peaks for the optimized nano-bilosomes formulation, indicating successful nano-encapsulation and the

presence of hydrogen bonding and van der Waals interactions, without any chemical incompatibility. These findings are clinically relevant as they confirm the physicochemical integrity of Levofloxacin during nano-bilosome incorporation, supporting its potential for controlled and stable nano-drug delivery. Similar spectral modifications suggesting successful entrapment and drug-matrix interactions were observed in nanostructured lipid carriers developed for Levofloxacin, which also

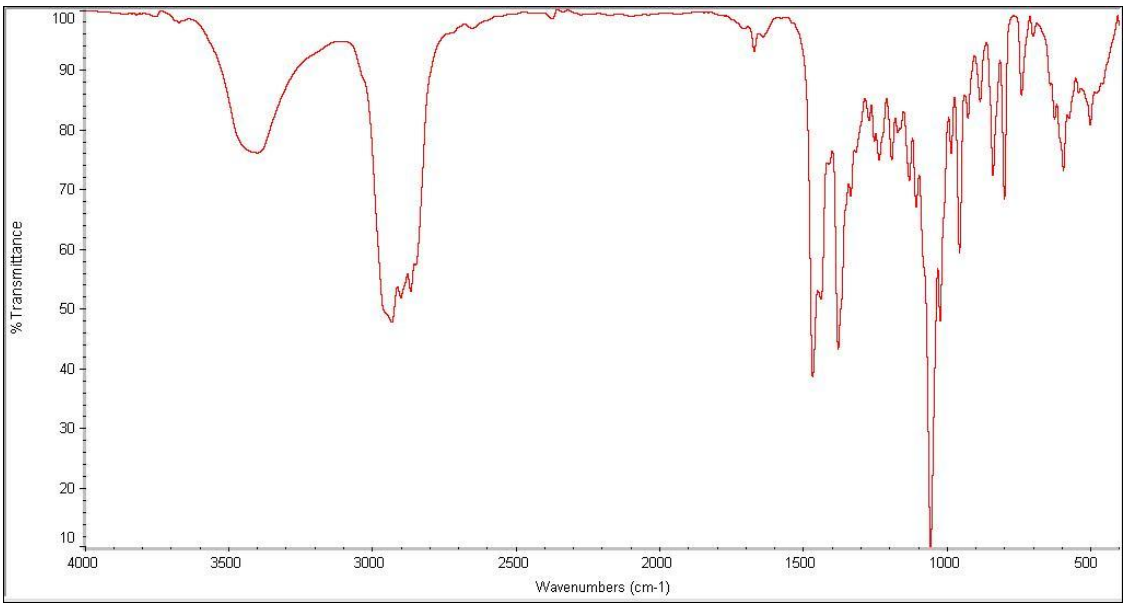

A

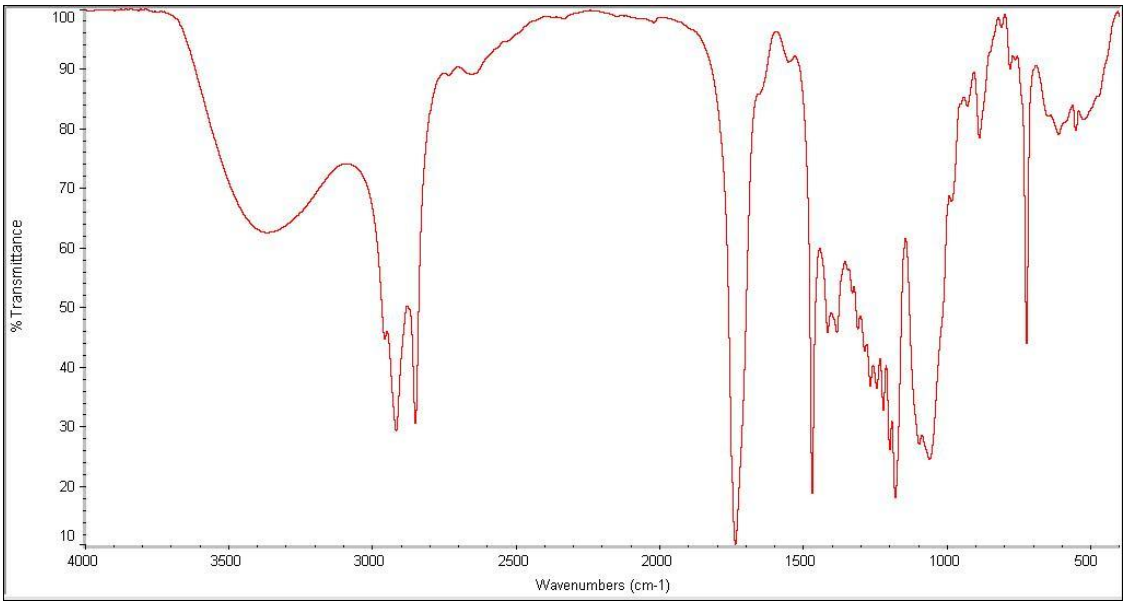

B

Fig. 7. Fourier Transform Infrared (FTIR) spectra of A) Cholesterol B) Span 60.

showed non-crystalline drug incorporation [31]. Another study also reported FTIR spectral changes like reduced carbonyl and OH peaks in Levofloxacin nanoparticles, confirming encapsulation and absence of drug degradation [23]. Furthermore, FTIR analysis of Levofloxacin and sulfamethoxazole-treated microalgae showed clear molecular-level interactions and alterations in protein and lipid content, reinforcing FTIR's sensitivity in detecting biochemical changes due to drug presence [32]. The comparison affirms that FTIR reliably detects intermolecular interactions in various Levofloxacin nano-formulations, supporting its utility in characterizing nano-encapsulation without

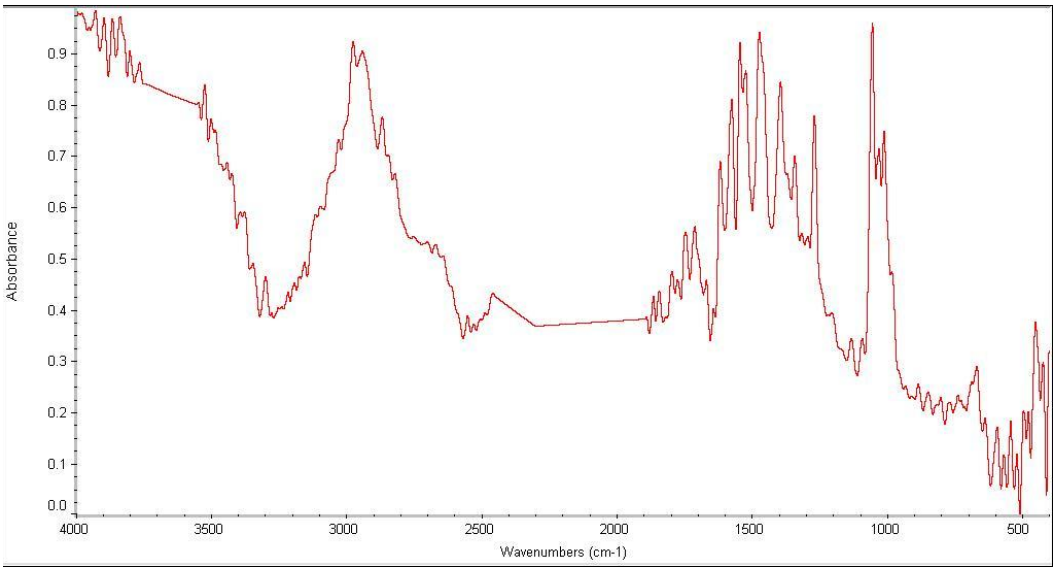

A

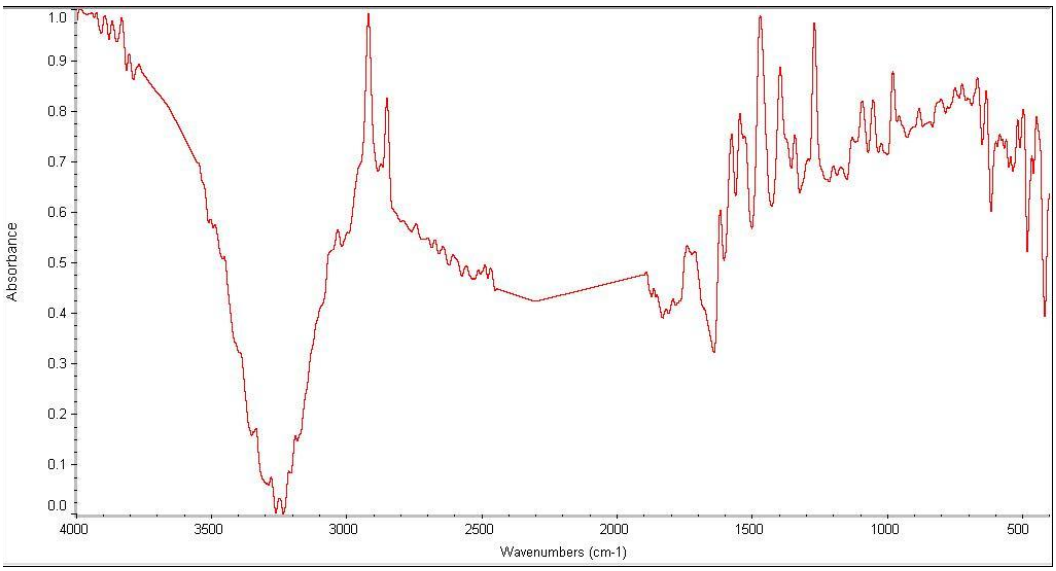

B

Fig. 8. Fourier Transform Infrared (FTIR) spectra of A) Physical mixture B) Optimized nanoscale bilosome formulation (F5).

compromising drug structure.

XRD: loss of sharp peaks → amorphization in nano-bilosomes

The XRD pattern of pure Levofloxacin (C) displayed multiple sharp and intense peaks, notably at 2θ ≈ 6°, 13°, 20°, and 26°, confirming its highly crystalline nature (Figs. 9-11). Similarly, Span 60 (A) and cholesterol (B) exhibited strong characteristic peaks between 18°–24° and 10°–23°, respectively,

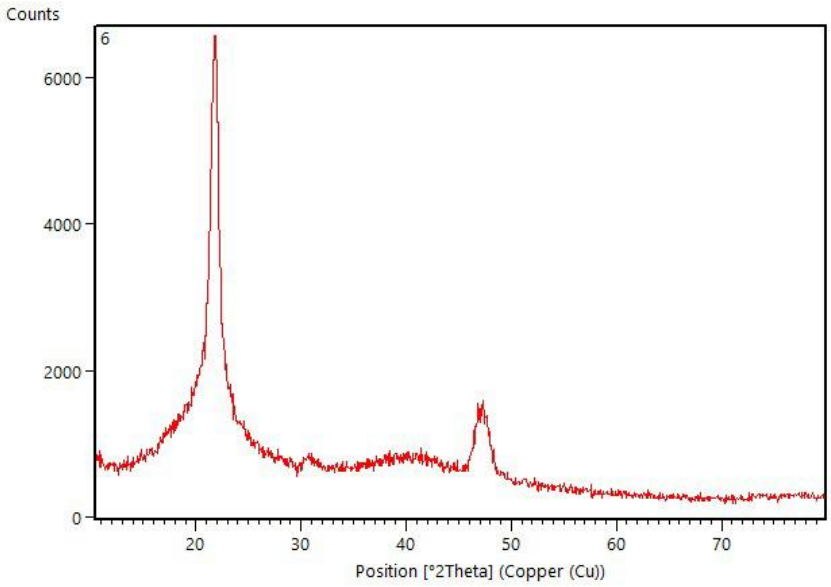

A

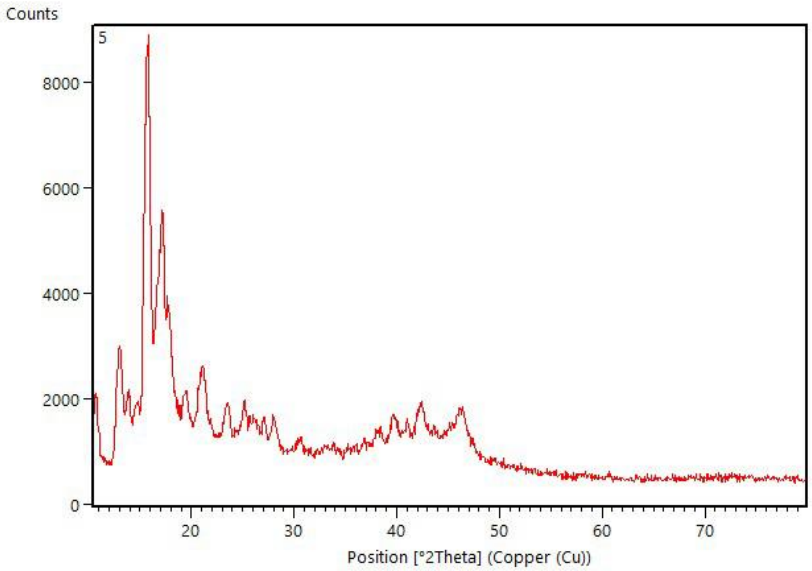

Fig. 9. Powder X-ray Diffraction (XRD) patterns A) Span 60 B) Cholesterol.

indicative of their semi-crystalline structures. Sodium deoxycholate (D) also showed a series of low-intensity but sharp peaks in the range of 15°–30°, supporting its partially crystalline character. In contrast, the physical mixture (E) retained most of the individual peaks of its components but

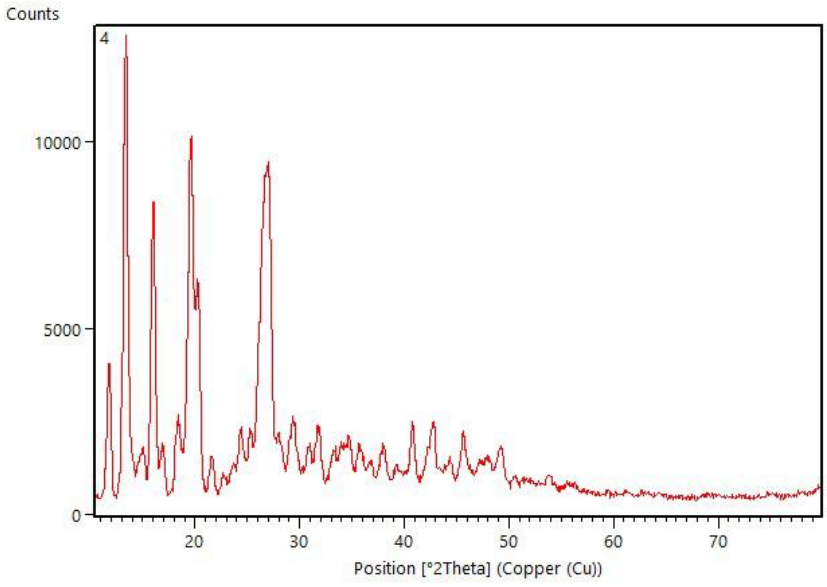

A

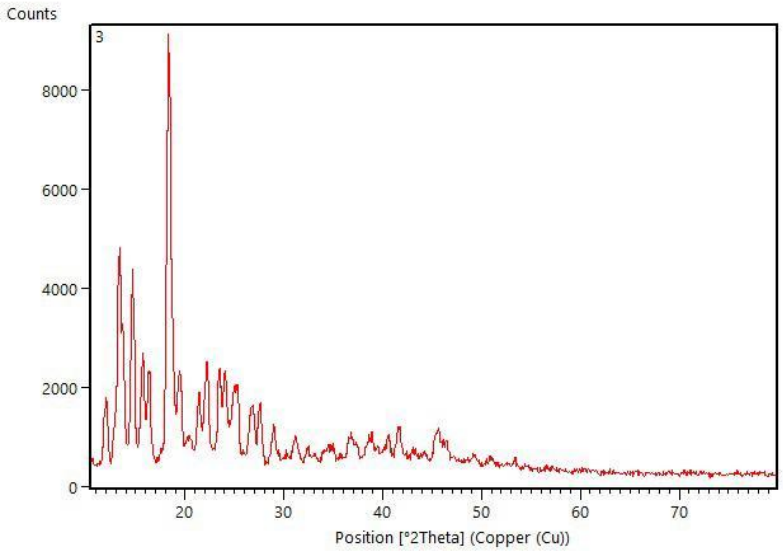

B

Fig. 10. Powder X-ray Diffraction (XRD) patterns A) Levofloxacin B) SDC.

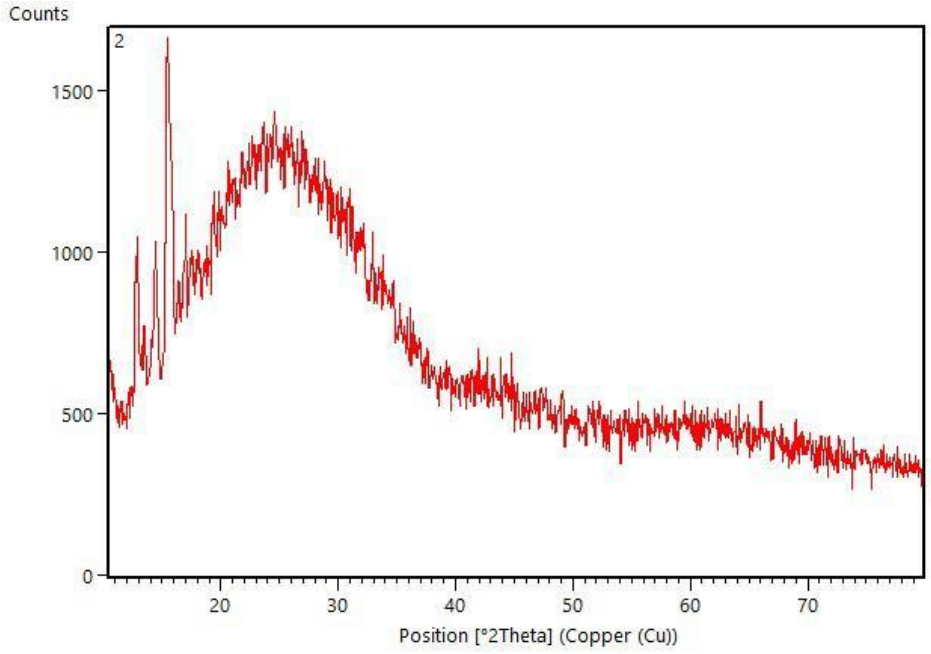

A

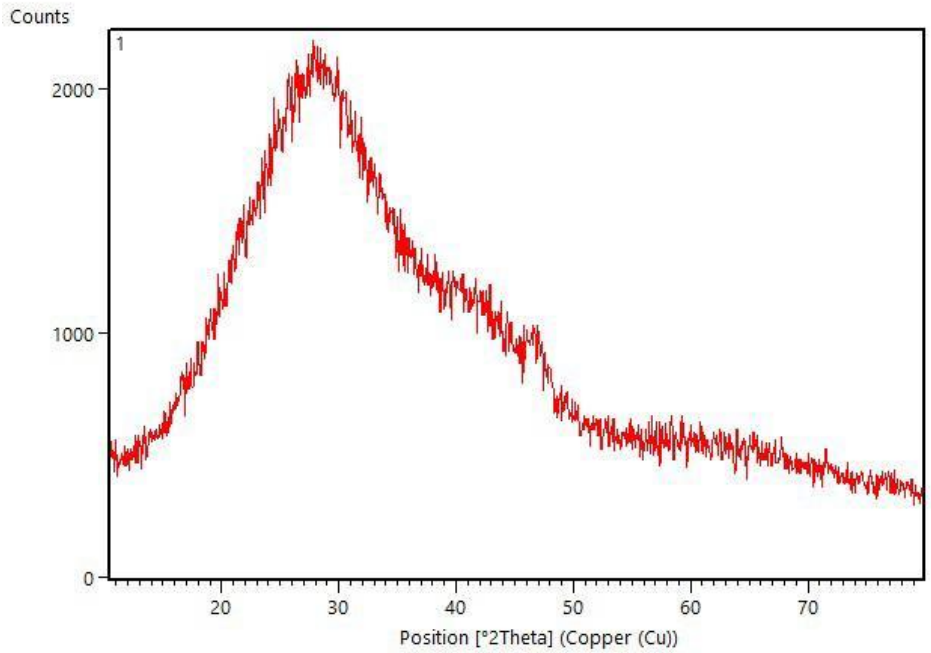

B

Fig. 11. Powder X-ray Diffraction (XRD) patterns A) Physical mixture B) Optimized nanoscale bilosome formulation (F5).

with noticeably reduced intensity, particularly for Levofloxacin and cholesterol. This suggests partial physical interaction or reduced crystalline order due to mixing. Notably, the XRD pattern of the optimized nano-bilosomes (F) showed a complete loss of sharp diffraction peaks and a broad diffuse halo, especially in the 2θ range of 15°–30°, characteristic of an amorphous or disordered nano-structure. The disappearance of Levofloxacin's sharp crystalline peaks confirms its successful nano-encapsulation within the lipid bilayer and its transformation from a crystalline to an amorphous state. This amorphization is a favorable outcome, as it is generally associated with enhanced solubility and potentially improved bioavailability of poorly water-soluble drugs. The absence of recrystallization peaks further indicates that Levofloxacin remains molecularly dispersed within the nano-bilosomes matrix and that the formulation method was effective in stabilizing the drug in its amorphous form. The present study demonstrated a complete amorphization of

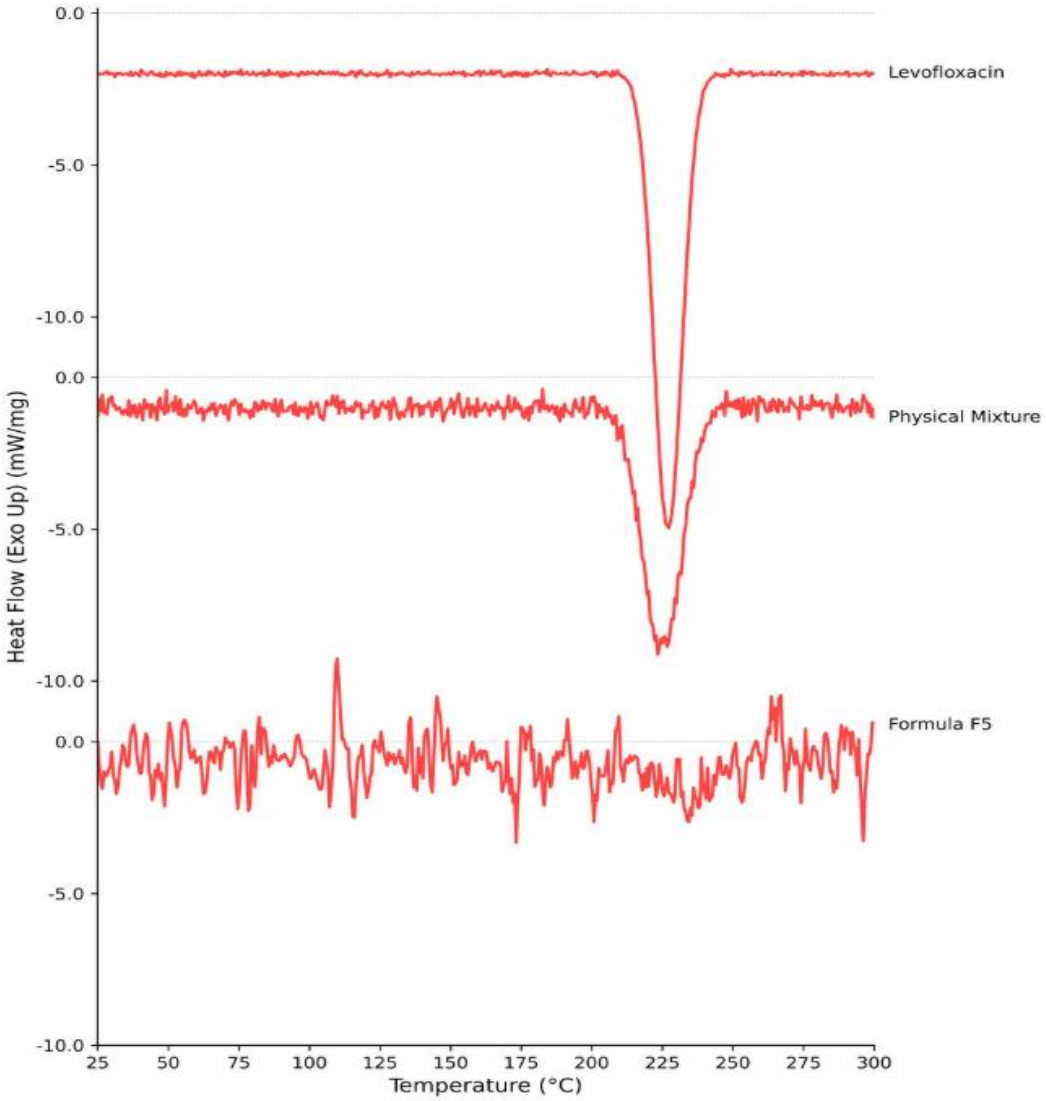

Fig. 12. Differential Scanning Calorimetry (DSC) thermograms of pure Levofloxacin, physical mixture, and the optimized nanoscale bilosome formulation (F5), confirming the loss of the characteristic drug endotherm and successful incorporation into the nanostructure.

Levofloxacin in the optimized nano-bilosomes, as confirmed by the disappearance of sharp peaks in the XRD pattern, indicating a transformation from a crystalline to an amorphous state. This transition suggests successful molecular dispersion of the drug within the nano-bilayer, which is associated with enhanced solubility and improved bioavailability—a key advantage in nano-drug delivery formulations [33].findings of the present study are consistent with recent research where Levofloxacin was converted to an amorphous state through co-amorphous salt formation with L-arginine for pulmonary nano-delivery; the study showed robust amorphization and maintained stability across variable processing parameters [34]. Similarly, Kulkarni et al. employed spray drying and microfluidization to encapsulate Levofloxacin in nanoparticles, also reporting a predominantly amorphous structure with favorable nano-particle properties and non-toxicity, reinforcing the therapeutic potential of such systems [23]. Another comparable study by Hayee et al. encapsulated Levofloxacin in polymeric nanoparticles using PLGA and chitosan, with XRD analysis confirming the amorphous nature of the drug. The nano-formulations showed stable entrapment and antibacterial activity, suggesting amorphization plays a key role in improving the drug's performance against resistant strains [29]. These studies reinforce the clinical importance of drug amorphization in lipid-based or polymeric nano-delivery systems, as achieved in the current study. The consistent XRD profiles across studies suggest a robust correlation between amorphous transitions and enhanced solubility, leading to improved pharmacokinetics and therapeutic outcomes.

Nano-Thermal Analysis of Levofloxacin

The DSC thermogram of pure Levofloxacin exhibited a sharp endothermic peak at approximately 225 °C, confirming its crystalline nature. The physical mixture presented two thermal events: a broad endothermic band around 60 °C, attributed to excipients, and a distinct melting peak at 225 °C, corresponding to Levofloxacin. In contrast, the bilosomal formulation showed only a broad, low-intensity endothermic depression around 220 °C, with the disappearance of the sharp melting peak. This shift and broadening indicate that the drug was successfully encapsulated within the bilosomal lipid matrix, leading to partial or complete amorphization, improved miscibility with excipients, and enhanced potential for dermal permeability (Fig. 12).

Stability: refrigerated retention of size/zeta/EE vs room-temp drift

Statistical analysis was performed using one-way ANOVA followed by Tukey's HSD post-hoc test to compare all groups with the initial baseline values. Values in bold indicate statistically significant differences ($p < 0.05$). The statistical results demonstrate significant physicochemical changes in the optimized nano-bilosomes stored at 25 °C over time, while samples maintained at 4 °C exhibited no significant variation. Nano-vesicle size, PDI, and zeta potential showed $p < 0.001$ after 3 months at room temperature, indicating nano-vesicle aggregation and reduced electrostatic stability. Entrapment efficiency (EE%) also declined significantly ($p < 0.001$), confirming partial drug leakage. Conversely, refrigerated samples retained consistent nano-size, charge, and EE%, confirming physical stability under cold storage. Overall, the

Table 2. Short-term stability profile of the optimized nanoscale bilosome formulation (F5) stored at 4 °C and 25 °C over 30 days, showing the change in key colloidal parameters (size, PDI, zeta potential, and EE%) and confirming superior stability under refrigerated conditions.

Time Point	Storage Temp.	Vesicle Size (nm) ± SD	p-value	PDI ± SD	p-value	Zeta Potential (mV) ± SD	p-value	EE (%) ± SD	p-value
Initial	—	93.0 ± 1.2	—	0.398 ± 0.01	—	–51.7 ± 0.8	—	91.0 ± 0.5	—
1 Month	4 °C	94.6 ± 1.4	0.219	0.403 ± 0.02	0.332	–51.3 ± 0.9	0.574	89.5 ± 0.6	0.078
1 Month	25 °C	105.3 ± 2.1	0.003	0.427 ± 0.02	0.012	–49.1 ± 1.1	0.008	85.6 ± 0.9	0.004
3 Months	4 °C	97.2 ± 1.8	0.089	0.418 ± 0.03	0.144	–50.5 ± 1.2	0.226	87.2 ± 0.7	0.041
3 Months	25 °C	128.4 ± 3.6	<0.001	0.481 ± 0.04	<0.001	–44.8 ± 1.6	<0.001	79.4 ± 1.3	<0.001

data statistically validate that low-temperature storage effectively preserves nano-bilosomes' integrity and entrapment capacity, supporting its recommendation for optimal nano-formulation stability.

CONCLUSION

This work establishes a composition–property map for levofloxacin-loaded nano-bilosomes and identifies an optimized formulation (F5) that combines nanoscale size, acceptable dispersity, a highly negative surface charge, and high entrapment. The data demonstrate a surfactant-driven reduction in nano-vesicle size up to a saturation threshold and a clear biphasic cholesterol effect, with ~100 mg delivering the best balance between bilayer rigidity and fluidity. Solid-state analyses verify noncovalent drug–excipient interactions without chemical incompatibility and confirm conversion of crystalline levofloxacin to an amorphous state within the nano-bilosomal matrix. Stability results support refrigerated storage (4 °C) to preserve nano-size, charge, and drug retention, while room-temperature storage (25 °C) leads to measurable aggregation and EE% loss over time. Collectively, these findings provide an experimentally validated route to stable, high-loading nano-bilosomes suitable for topical antibiotic delivery and justify subsequent ex vivo skin permeation, microbiological performance, and in vivo efficacy/safety studies.

CONFLICT OF INTEREST

The authors declare that there is no conflict of interests regarding the publication of this manuscript.

REFERENCES

1. Millar BC, McCaughan J, Rendall JC, Moore JE. Delafloxacin––A novel fluoroquinolone for the treatment of ciprofloxacin-resistant Pseudomonas aeruginosa in patients with cystic fibrosis. The Clinical Respiratory Journal. 2020;15(1):116-120.
2. Berry L, Domalaon R, Brizuela M, Zhanel GG, Schweizer F. Polybasic peptide–levofloxacin conjugates potentiate fluoroquinolones and other classes of antibiotics against multidrug-resistant Gram-negative bacteria. MedChemComm. 2019;10(4):517-527.
3. Hassanshahi G, Darehkordi A, Sheikh Fathollahi M, Khanamani Falahati-Pour S, Rezazadeh Zarandi E, Assar S. Resistance pattern of Escherichia coli to levofloxacin in Iran, a narrative review. Iranian Journal of Microbiology. 2020.
4. Qiao M, Ren W, Guo H, Huo F, Shang Y, Wang Y, et al. Comparative in vitro susceptibility of a novel fluoroquinolone antibiotic candidate WFQ-228, levofloxacin, and moxifloxacin against Mycobacterium tuberculosis. Int J Infect Dis. 2021;106:295-299.
5. Carvalhaes CG, Shortridge D, Duncan LR, Huband M, Castanheira M. 2754. Delafloxacin and Comparator Fluoroquinolone In Vitro Resistance Trends in Isolates from Skin and Skin Structure Infections in the USA (2017–2022). Open Forum Infectious Diseases. 2023;10(Supplement_2).
6. Mitrović D, Zaklan D, Đanić M, Stanimirov B, Stankov K, Al-Salami H, et al. The Pharmaceutical and Pharmacological Potential Applications of Bilosomes as Nanocarriers for Drug Delivery. Molecules. 2025;30(5):1181.
7. Mondal D, Mandal RP, De S. Addressing the Superior Drug Delivery Performance of Bilosomes–A Microscopy and Fluorescence Study. ACS Applied Bio Materials. 2022;5(8):3896-3911.
8. Sharma B, Chauhan I. A Review: Bilosomes as Nanocarriers. Current Nanomedicine. 2024;14(3):178-187.
9. Aralelimath K, Sahoo J, Wairkar S. Dermal drug delivery via bilosomes: a synergistic integration for better therapeutic outcomes. Journal of Microencapsulation. 2024;41(8):818-831.
10. Palekar-Shanbhag P, Lande S, Chandra R, Rane D. Bilosomes: Superior Vesicular Carriers. Curr Drug Ther. 2020;15(4):312-320.
11. Maharini I, Martien R, Nugroho AK, Supanji S, Adhyatmika A. Validation UV Spectrophotometric Method to Determine Entrapment Efficiency of Ocular Polymeric Nanoparticle Levofloxacin Hemihydrate. Research Journal of Pharmacy and Technology. 2021:5479-5482.
12. Üçer A, Ertekin ZC, Dinç E. A comparative application of spectrophotometric and spectrofluorimetric methods to estimate levofloxacin-DNA and ofloxacin-DNA interactions. Journal of Fluorescence. 2024;35(8):6937-6946.
13. Adachi K, Shimizu M, Shono F, Funatsu K, Yamazaki H. Octanol/water partition coefficients estimated using retention times in reverse-phase liquid chromatography and calculated in silico as one of the determinant factors for pharmacokinetic parameter estimations of general chemical substances. The Journal of Toxicological Sciences. 2024;49(4):127-137.
14. Abdelbary AA, Abd-Elsalam WH, Al-mahallawi AM. Fabrication of novel ultradeformable bilosomes for enhanced ocular delivery of terconazole: In vitro characterization, ex vivo permeation and in vivo safety assessment. Int J Pharm. 2016;513(1-2):688-696.
15. Garg S, Patel P, Gupta GD, Kurmi BD. Pharmaceutical Applications and Advances with Zetasizer: An Essential Analytical Tool for Size and Zeta Potential Analysis. Micro and Nanosystems. 2024;16(3):139-154.
16. Seçilmiş Canbay H, Doğantürk M. Application of Differential Scanning Calorimetry and Fourier Transform Infrared Spectroscopy to the Study of Metoprolol-Excipient and Lisinopril-Excipient Compatibility. Eurasian Journal of Analytical Chemistry. 2018;13(5).
17. Abdel Salam L, Abdelmottaleb M, Geneidi A. Formulation and Characterization of Proniosomal Gels loaded with Levofloxacin for dermal drug Delivery. Archives of Pharmaceutical Sciences Ain Shams University. 2021;5(2):288-303.
18. Agha OA, Girgis GNS, El-Sokkary MMA, Soliman OAE-A. Spanlastic-laden in situ gel as a promising approach for ocular delivery of Levofloxacin: In-vitro characterization, microbiological assessment, corneal permeability and in-vivo study. International Journal of Pharmaceutics: X. 2023;6:100201.
19. Shinde U, Barkat Y, Singh K. Coloaded Surface–Modified PLGA

Nanoparticles for Sustained Ocular Delivery of Levofloxacin and Flurbiprofen. J Pharm Innov. 2023;18(4):2348-2361.
20. Ali SK, Entidhar JA-A. Bilosomes as Soft Nanovesicular Carriers for Ropinirole Hydrochloride: Preparation and In- vitro Characterization. Iraqi Journal of Pharmaceutical Sciences(P-ISSN 1683 - 3597 E-ISSN 2521 - 3512). 2023;32(Suppl.):177-187.
21. Kulkarni V, Sonawane L, No author Na, Kalyanka T, Kshirsagar R. Preparation and Characterization of Levofloxacin Hemihydrate Laden Spray Dried Nanoparticles through Micro fluidization for Drug Delivery. Journal of Complementary Medicine Research. 2022;13(4):130.
22. Abdelatif HA, Ahmed HI, Sherif Kh. Abu-El Y, Ahmed MS. Design, Formulation, and In-Vitro Characterization of Lipid-Based Nano-Bilosomal Vesicles of Lovastatin. Universal Journal of Pharmaceutical Research. 2025.
23. Nasri S, Ebrahimi-Hosseinzadeh B, Rahaie M, Hatamian-Zarmi A, Sahraeian R. Thymoquinone-loaded ethosome with breast cancer potential: optimization, in vitro and biological assessment. Journal of Nanostructure in Chemistry. 2020;10(1):19-31.
24. Naji GH, Al Gawhari FJ. Figure 1 from: Naji GH, Al Gawhari FJ (2024) Evaluation of types and concentration of bile salts impact on physical properties of nisoldipine-loaded bilosomes. Pharmacia 71: 1-7.
25. Holsæter AM, Wizgird K, Karlsen I, Hemmingsen JF, Brandl M, Škalko-Basnet N. How docetaxel entrapment, vesicle size, zeta potential and stability change with liposome composition–A formulation screening study. Eur J Pharm Sci. 2022;177:106267.
26. Banerjee KK, Maity P, Das S, Karmakar S. Effect of cholesterol on the ion-membrane interaction: Zeta potential and dynamic light scattering study. Chemistry and Physics of Lipids. 2023;254:105307.
27. Hayee R, Iqtedar M, Albekairi NA, Alshammari A, Makhdoom MA, Islam M, et al. Levofloxacin loaded chitosan and poly-lactic-co-glycolic acid nano-particles against resistant bacteria: Synthesis, characterization and antibacterial activity. Journal of Infection and Public Health. 2024;17(5):906-917.
28. Beraldo-Araújo VL, Flávia Siqueira Vicente A, van Vliet Lima M, Umerska A, Souto EB, Tajber L, et al. Levofloxacin in nanostructured lipid carriers: Preformulation and critical process parameters for a highly incorporated formulation. Int J Pharm. 2022;626:122193.
29. Islan GA, Tornello PC, Abraham GA, Duran N, Castro GR. Smart lipid nanoparticles containing levofloxacin and DNase for lung delivery. Design and characterization. Colloids Surf B Biointerfaces. 2016;143:168-176.
30. Xiong Q, Liu Y-S, Hu L-X, Shi Z-Q, Ying G-G. Levofloxacin and sulfamethoxazole induced alterations of biomolecules in Pseudokirchneriella subcapitata. Chemosphere. 2020;253:126722.
31. Kadri L, Casali L, Emmerling F, Tajber L. Mechanochemical comparison of ball milling processes for levofloxacin amorphous polymeric systems. Int J Pharm. 2024;665:124652.
32. Gabelmann A, Lehr C-M, Grohganz H. Preparation of Co-Amorphous Levofloxacin Systems for Pulmonary Application. Pharmaceutics. 2023;15(6):1574.